Pergamon

J. Aerosol Sci., Vol. 26, No. 3, pp. 353–367, 1995

0021-8502/95 $9.50 + 0.00

0021-8502(94)00093-X

AEROSOL PENETRATION THROUGH CAPILLARIES AND LEAKS: EXPERIMENTAL STUDIES ON THE INFLUENCE OF PRESSURE

D. A. V. Morton* and J. P. Mitchell†

Aerosol Science Centre, AEA Technology, Winfrith, Dorchester, Dorset DT2 8DH, U.K.

(*First received* 25 *February* 1994; *and in final form* 30 *May* 1994)

Abstract—It is important to understand the movement of aerosols through ultrafine leak-paths with dimensions of similar order to the gas-borne particles when assessing the validity of leak-testing procedures for transport containers for radioactive materials. Experiments have been undertaken to investigate the penetration of micron-sized airborne particles using glass micro-capillaries as model leak-paths. Previous studies demonstrated a simple relationship between air leakage and total particle penetration rates at a constant driving pressure (100 kPa). The present work has demonstrated the importance of pressure in regulating the rate at which the leak-path is plugged by deposited particles. Much of this deposition appears to take place at the entrances of the capillaries where the air-flow converges.

INTRODUCTION

The transport and storage of radioactive materials requires the use of specialised containers that must be shown to be leak-tight to certain standards. These standards are determined by the type of radioactive material being contained and the potential hazards from the release of such radionuclides (IAEA, 1985). In addition, the U.K. Atomic Energy Code of Practice describes methods for the leakage testing of transport and storage packages (AEA Technology, 1992). Containers for large quantities of radioactive material are tested for compliance with these standards before being released for dispatch or storage. The leakage testing of containers for radioactive materials is a time-consuming process, particularly, if it is necessary to detect very low gas leakage rates in order to demonstrate compliance with the necessary regulations. It is therefore advantageous to the user of these containers if it can be demonstrated that fine particle leakage does not occur at gas leakage rates that can be measured easily and cheaply.

In assessments of particle leakage, the conservative assumption is usually made that the particles will penetrate the leak-path if the assessed size distribution includes a significant proportion of particles with diameters less than the maximum hole size. Experimental work undertaken by Curren and Bond (1980) indicated that the blockage of critical orifice type leak-paths will occur if a significant number of particles have diameters greater than that of the leak aperture. This process will obviously prevent any further leakage of particles from the container. Other assumptions are also made when assessing and quantifying particle leakage across a damaged container seal. For instance, the total leakage is attributed to a single pathway, which is assumed to have a circular profile. Furthermore, aerosol is assumed to exist under pressure within the container, which implies that mechanisms must operate within the gas space to entrain such particles and to develop the excess pressure in the first place. This conservative approach almost certainly results in gross over-estimates of the quantities of radioactive aerosol that would be released into the environment under accident conditions. Hence, it is important to quantify aerosol leakage rates, as well as identify limiting features such as particle blockage of the leak-path, in order to optimise costs, and avoid unnecessary failures during routine container leak-testing.

* Author to whom correspondence should be addressed.
† Present address: Trudell Medical, London, Ont., Canada N5Z 3M5.

During the past three years, a programme of work has been undertaken by the Aerosol Science Centre at Winfrith to quantify the leakage of airborne particles through well-defined leak-paths based on micro-capillaries (Mitchell *et al.*, 1990; Burton *et al.*, 1993). This work has concentrated mainly on the behaviour of ultra-fine capillaries, chiefly in the range 10–50 μm internal diameter and 5–50 mm in length. The geometries of actual leak-paths are uncertain, the most likely scenario being a curved gap between the 'O'-ring and the metal surfaces on which it locates, perhaps caused by a crack or cut in the elastomeric material from which these seals are made. The choice of a capillary as the model leak-path was an attempt to understand particle penetration behaviour under worst-case conditions (i.e. a straight leak-path).

The flow of air through such leak-paths is laminar rather than turbulent when the driving pressure is equal or less than 100 kPa (Mitchell *et al.*, 1990). In the initial experiments, the aerosol particles comprised glass spheres in the size range from approximately 2–20 μm volume equivalent diameter. Later, these smooth-surfaced particles were replaced with similar sized irregular-shaped cerium oxide particles as simulants for irradiated materials such as uranium or plutonium oxides, since it was believed that such particles are more likely to stick to each other as well as the walls of the capillary, thereby reducing particle leakage rates. Such behaviour did not occur to a significant extent (Morton *et al.*, 1992; Mitchell *et al.*, 1992), and subsequent work was therefore undertaken with the original glass microspheres, which are a well-characterised secondary reference material of known shape, density and size distribution (Ball *et al.*, 1989). All of these experiments were undertaken with the objective of correlating particle penetration with air leakage, which is the main parameter that is measurable during the routine leak testing of transport containers.

The present paper is concerned with the latest series of experiments in which the pressure differential across the capillary leak-path was varied from 20 to 100 kPa. The experimental work undertaken to date forms a sound basis on which useful predictions can be made of the likelihood that significant aerosol leakage will occur when containers are tested in accordance with current and future regulations (Stopford and Williams, 1992; Clement, 1993). It should be noted that the findings may also have implications in the treatment of aerosol leakage in a variety of non-nuclear applications, including the integrity of valves and fittings for the supply of particle-free gases as well as the containment of particles in pressurised environments.

EXPERIMENTAL PROCEDURES

All of the experiments were based on the measurement of air and particle leakage rates through micro-capillary tubes made from borosilicate glass. Their preparation, sizing and testing with the equipment used to measure leakage of particle-free air before and after aerosol exposure have been described elsewhere (Mitchell *et al.*, 1990). In the present studies, the capillaries were similar, varying from 19 to 21 mm in length and from 28 to 35 μm in bore.

Air leakage testing

The leak-tightness of a containment vessel is determined by measuring the leakage rate of a test fluid (air in the present studies) leaking to or from the vessel under known conditions of temperature, upstream and downstream pressure (pressure differential) and gas viscosity. It is convenient in comparisons of leakage behaviour to obtain standardised leakage rates (SLRs) by reference to commonly agreed conditions outside the vessel, such as pressure (P_S) = 100 kPa, temperature (T_S) = 298 K and air viscosity (μ_S) of 1.85×10^{-5} kg m^{-1} s^{-1} (AEA Technology, 1992).

In the present study, the SLR for each capillary was determined by measuring the increase in pressure of a chamber located downstream. The chamber was initially evacuated to a pressure less than 10 kPa, and the subsequent rise in pressure monitored while admitting particle-free air into the system (Fig. 1). The operation of this equipment has already been

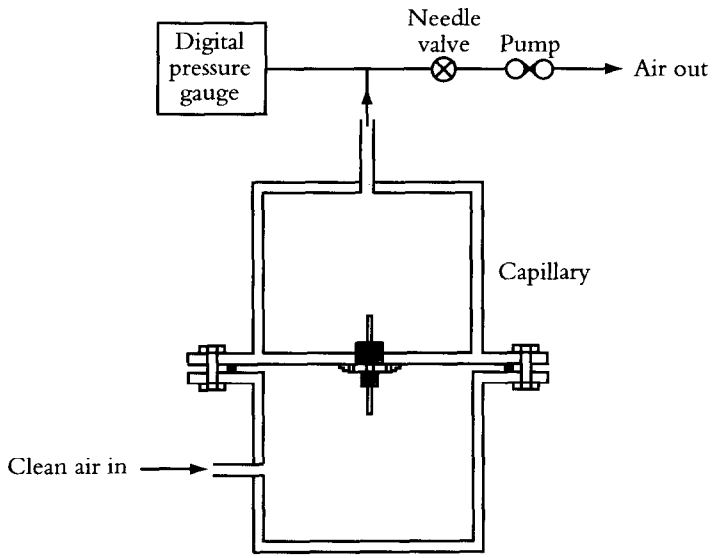

Fig. 1. Apparatus for the determination of capillary leak-rates.

described (Mitchell *et al.*, 1990); the system is capable of detecting air leakage rates having SLR values as low as 10^{-7} Pa m^3 s^{-1}. The SLR was calculated from the rise in pressure from an initial value (P_1) to the final pressure (P_2) during the period H, using the equation:

$$\mathrm{SLR} = \frac{VT_s}{HT_a}(P_1 - P_2)\left[\frac{\mu_a(P_s^2 - P_0^2)}{\mu_s(P_u^2 - P_d^2)}\right], \quad (1)$$

in which V is the volume of the partly evacuated chamber (3.32×10^{-4} m^3), T_a and μ_a are the actual air temperature and viscosity, respectively, P_0 is zero pressure and P_u and P_d are the capillary entrance (upstream) and exit (downstream) pressures, respectively. At the start of the measurements P_u and P_d were <10 and 100 kPa, respectively.

Aerosol exposure

All of the aerosol exposure experiments were undertaken using micron-sized glass microspheres (product GS5000, Whitehouse Scientific Ltd., Waverton, Chester, U.K.). The aerosol was generated using the fluidised-bed technique of Marple *et al.* (1978), modified to operate at air pressures in excess of atmospheric pressure (Fig. 2). The detailed operating principle has been described elsewhere (Mitchell *et al.*, 1990); in these studies the maximum aerosol concentration attainable was increased over two orders of magnitude to more than 10^{10} particles m^{-3} by supplying additional glass powder to the fluidised-bed as well as increasing the flow of air through the bed. At the same time, the effective volume of the aerosol pressure chamber was reduced by an order of magnitude by inserting a narrow, cylindrical Perspex sleeve on-axis with the capillary. The modification resulted in a more efficient recirculation of the aerosol by eliminating horizontal surfaces that had previously removed air-borne particles from the system due to gravitational settling. These changes resulted in a marked improvement in the stability of the aerosol in the chamber; nevertheless the mass concentration decreased by approximately an order of magnitude during the first hour following the initial burst of particles as the fluidised-bed was started up. Although desirable, electrical charge equilibration of the aerosol was not attempted in view of the operational/regulatory difficulties in installing a radioactive source in the pressurised container.

In previous work, the mounting plate for the capillary on test had been fabricated from Perspex, but it was noted that the screw-thread into which the capillary support was secured was susceptible to wear, with the result that on occasions parasitic leak-paths developed,

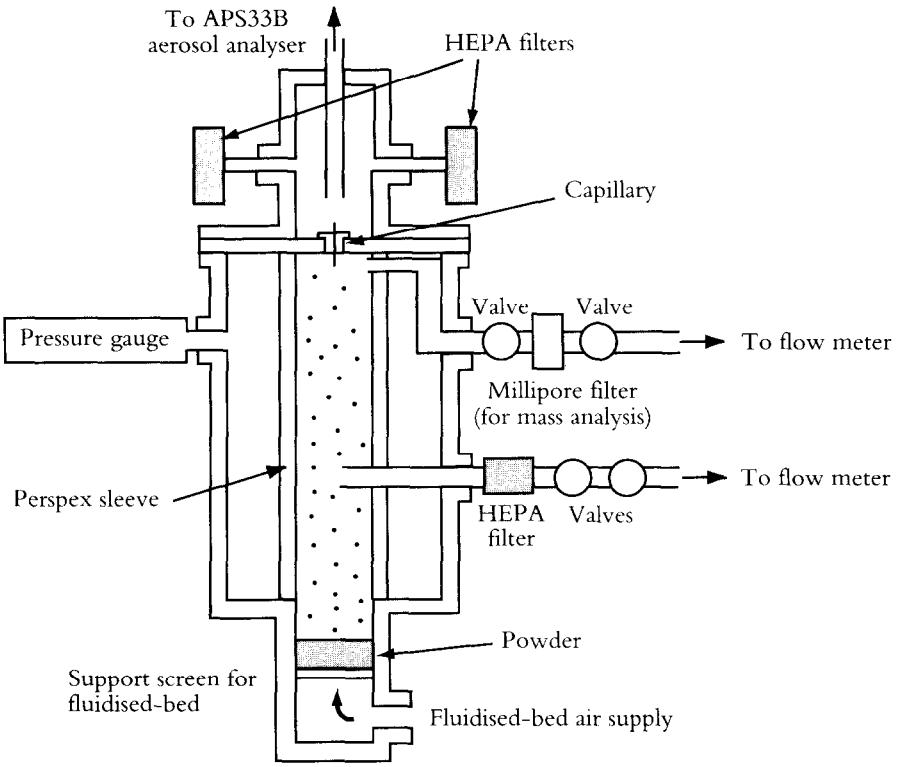

Fig. 2. Apparatus for aerosol exposure and penetration measurements.

rendering the particle penetration data invalid. This plate was replaced with one fabricated from stainless steel, and a thin layer of silicone rubber sealant was located around the capillary support mounting on the plate to ensure the integrity of the seal.

Measurements of the number-aerodynamic size distribution of the airborne particles in the pressure chamber (in this case operating at ambient pressure) by a real-time Aerodynamics Particle Sizer (model APS33B, TSI Inc., St. Paul, Minnesota, U.S.A. (Remiarz *et al.*, 1983)) confirmed that the aerosol was moderately polydisperse, with a count median aerodynamic diameter (CMAD) close to 4 μm and geometric standard deviation (σ_g) of 1.9 (Fig. 3). The count median geometric diameter (CMGD) was based on the volume equivalent diameter and obtained by microscopy-image analysis: the resulting value was slightly smaller than the CMAD of 3.0 μm (Ball *et al.*, 1989). These particles were representative in aerodynamic terms of uranium/plutonium oxide particles that might be aerosolised during transport of these materials (Current and Bond, 1980).

Each capillary on test was exposed to the glass microsphere aerosol generated in the main chamber which had a pre-set pressure in the range $20-100 \pm 1$ kPa above room ambient. The outflow of air from side-vents in the aerosol chamber was restricted by needle-valves so that the upstream pressure at the capillary entrance could either be maintained at the predetermined level for the duration of each test, or adjusted to a new level during the course of experiments so that the capillary could be exposed to variations in the pressure differential in a systematic way.

During the course of each experiment, the aerosol mass concentration in the exposure chamber was repeatedly determined by sampling the airborne particles directly from the chamber atmosphere onto a Millipore membrane filter (type GS, 0.22 μm porosity, Millipore Corp., Bedford, Massachusetts, U.S.A.) at a volumetric flow rate of 5 l min^{-1} for 5–15 min periods depending on the aerosol concentration, followed by gravimetric analysis. These mass concentration data were required to compensate for the decreasing aerosol concentration in the pressure vessel, when comparing particle penetration rates made during

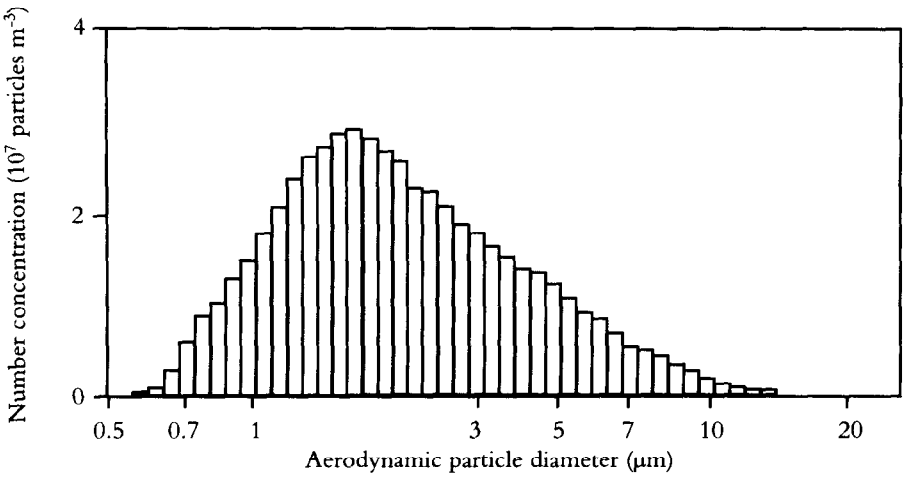

Fig. 3. APS33B-measured size distribution for GS5000 glass microspheres.

the course of each capillary exposure test. The sampling point for the mass concentration measurements was located within the aerosol chamber at the same level as the capillary in order to obtain representative samples, but at sufficient distance from the capillary to avoid interference with aerosol movement near to the capillary entrance. Care was taken to avoid altering the pressure differential across the capillary leak-path during the time when aerosol samples were extracted to the filter sampler.

The mass concentration of aerosol that penetrated the capillary on test was too small to be determined by the filter-collection method; a single-particle detector was required to provide the sensitivity needed, particularly when penetration rates were at their lowest. An APS33B was therefore used to sample the outflow from the capillary exit in a way that avoided disturbing the flow through the capillary (Fig. 4); the validation of this technique has already been described elsewhere (Mitchell *et al.*, 1990). It should be noted that particle penetration rates were obtained on a number-weighted basis because the APS33B is a single particle detector.

The particle penetration index (P_x) through the capillary at a particular time was obtained directly from the ratio of APS33B (N_{APS33B}) and filter-based (M_{FILTER}) measurements:

$$P_x = \frac{N_{\mathrm{APS33B}}}{M_{\mathrm{FILTER}}}. \tag{2}$$

It is noted that the dimensionless penetration efficiency could have been obtained by comparing the ratio of aerosol mass concentrations upstream and downstream of the capillary on test. However, such an approach would have given rise to large statistical errors associated with the conversion of the APS33B-measured number-weighted size distribution to a mass-weighted basis for the polydisperse aerosol being measured (Hinds, 1982). For this reason, no attempt has been made to determine absolute penetration efficiencies in these studies; instead, the P_x values were used to follow relative changes in penetration behaviour during the course of each test. The highest value of P_x (generally obtained at the start of each test) was therefore set to unity, and subsequent data for that test were normalised to permit comparisons to be made of particle penetration during the course of the exposure.

Post-aerosol exposure examination

The capillary was carefully removed from the facility after aerosol exposure, are re-mounted in the vacuum chamber to obtain the post-test air leakage rate. Finally, the capillary was inspected using an optical microscope to look for evidence of any particle deposits near to the entrance.

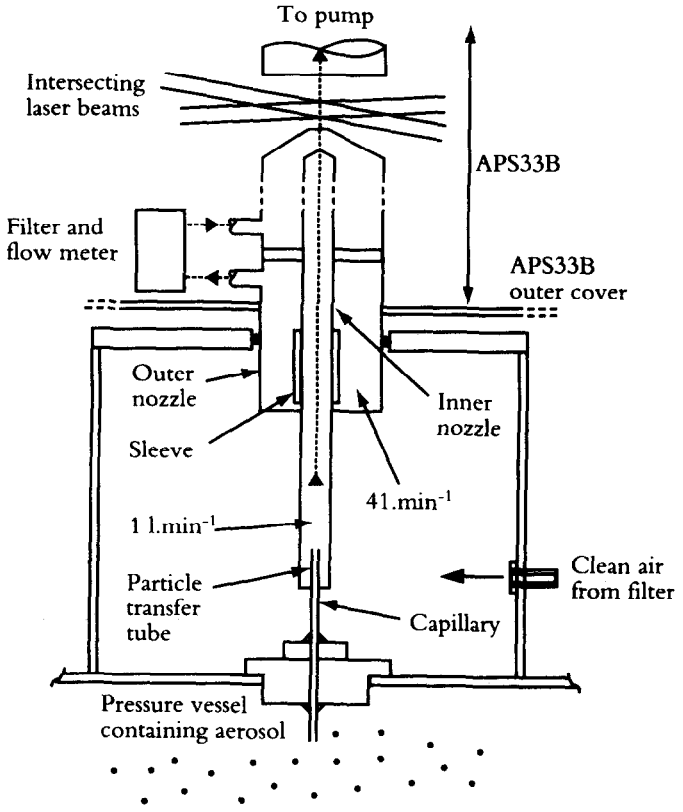

Fig. 4. Sampling arrangement for the APS33B.

Table 1. Measured and predicted air leakage rates for 20 mm long capillaries

Capillary number	Bore, d (μm)	SLR_{before} (Pa m^3 s^{-1})	SLR_{after} (Pa m^3 s^{-1})	SLR_p (Pa m^3 s^{-1})
1	29	2.0×10^{-4}	1.2×10^{-4}	2.34×10^{-4}
2	31	2.9×10^{-4}	2.8×10^{-4}	3.06×10^{-4}
3	31	3.3×10^{-4}	3.3×10^{-4}	3.06×10^{-4}
4	31	3.6×10^{-4}	3.6×10^{-4}	3.06×10^{-4}
5	29	2.2×10^{-4}	1.8×10^{-4}	2.34×10^{-4}
6	32	8.9×10^{-4}	3.4×10^{-4}	3.47×10^{-4}
7	29	1.3×10^{-4}	3.4×10^{-4}	2.34×10^{-4}
8	31	4.1×10^{-4}	7.1×10^{-5}	3.06×10^{-4}

RESULTS

Air leakage behaviour

SLR measurements made before (SLR_{before}) and after (SLR_{after}) aerosol exposure for each capillary are listed in Table 1, together with the predicted air leakage rate (SLR_p (Pa m^3 s^{-1})), based on the expression derived from Poiseuille's law for laminar flow (Burrows, 1961; AEA Technology, 1992):

$$SLR_p = 10^{-5}(P_u - P_d)\left[\frac{kd^4(P_u - P_d)}{2\mu_a b}\right]\left[\frac{\mu_a(P_s^2 - P_0^2)}{\mu_s(P_u^2 - P_d^2)}\right], \quad (3)$$

where k is a numerical constant (2.45×10^{-23}) which is valid for a smooth-walled tube, independent of gas type in laminar flow when the SLR is greater than 10^{-8} Pa m^3 s^{-1}. d is

Table 2. Pressure variations during aerosol exposure tests

Capillary number	Bore (d) (μm)	Pressure differential during aerosol exposure (kPa)
1	29	20 (fixed)
2	31	40 (fixed)
3	31	60 (fixed)
4	31	80 (fixed)
5	29	20 rising to 60
6	32	20 rising to 100
7	29	100 falling to 40
8	31	100 falling to 40

the capillary bore (μm), b the capillary length (mm) and μ_a is the air viscosity (kg m^{-1} s^{-1}). It should be noted that this expression does not take into account the effect that wall roughness may have on air flow through the leak-path.

Agreement between measured and predicted air leakage rates was generally good, considering the sensitivity of leakage to the magnitude of the capillary bore. The reduction in SLR after aerosol exposure is also significant; the largest changes were seen in cases where the capillary had been exposed to aerosol at relatively low pressure differential values of less than 60 kPa (see Table 2 for capillaries 1, 7 and 8). The reason for the anomalously high SLR_{before} for capillary 6 is not known.

Aerosol exposure

The first series of tests was performed at fixed upstream pressure in the range 20–80 kPa (Table 2), with the initial aerosol mass concentration in the pressure chamber varying from 1 to 3 g m^{-3}, and decreasing to about 10% of these values after 1 h. This behaviour is illustrated in Fig. 5 for the test where the pressure differential across the capillary was fixed at 80 kPa for 2 h.

The time-dependent variation of P_x is shown in Fig. 6 for capillaries tested at various fixed values of pressure differential. In experiment at 80 kPa, values of P_x remained above 0.4 for the duration of exposure, and was in the range 0.7–0.9 for most of the time, as shown in Fig. 6, curve (a). This capillary therefore remained largely un-plugged during the test. The pressure differential was next fixed at 60 kPa, and the particle penetration behaviour was observed with a new (clean) capillary. Values of P_x declined steadily, eventually decreasing to zero after 70 min, as shown in Fig. 6, curve (b). This capillary was almost completely plugged at the end of the test. When the pressure differential across the next capillary was reduced still further to 40 kPa, P_x decreased more rapidly than in the previous experiment, eventually reaching a value close to 0.15 when the test was terminated after 60 min (curve (c) of Fig. 6). Finally, three separate tests were undertaken at the lowest pressure differential investigated (20 kPa); in all cases, the capillaries plugged within the first 10 min of aerosol exposure (curve (d) of Fig. 6).

In a subsequent series of experiments, the chamber pressure was varied in a systematic way to see if partly or fully plugged capillaries could be unblocked by subsequent changes in upstream conditions (Table 2). In the first test, the pressure differential was increased in two steps from 20 to 60 kPa by 20 kPa increments at 30 and 50 min after starting capillary exposure to the aerosol. Figure 7(a) illustrates the pressure variation and associated changes in particle penetration efficiency, and the relationship between upstream and downstream particle concentration measurements during this experiment are shown in Fig. 7(b). The capillary blocked very rapidly at 20 kPa, as expected from the previous studies; however a small and temporary surge of particles was observed for a short time after the pressure had been increased to 40 kPa. No further penetration was observed following the final pressure increase to 60 kPa, and an attempt to dislodge the plug by increasing the pressure to 100 kPa was unsuccessful. Particle surges following pressure increments were also evident in a repeat

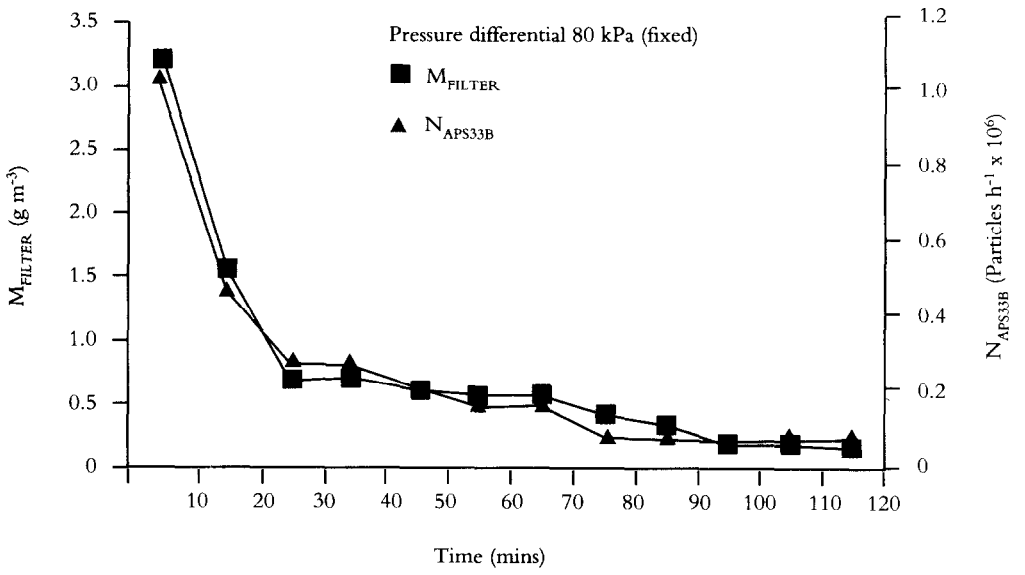

Fig. 5. Typical variation of aerosol concentration during 2 h test period.

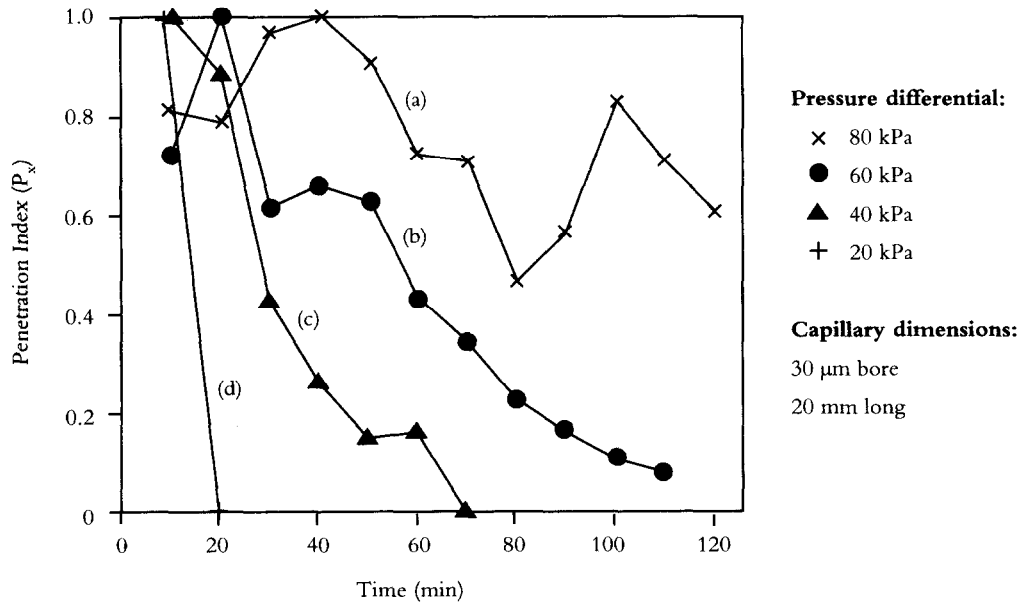

Fig. 6. Time-dependent variation of aerosol penetration.

test in which the pressure differential was increased to 100 kPa in 20 kPa steps (Fig. 7(a)). Plugs that had formed after 30, 70 and 100 min were temporarily cleared by the subsequent increases in chamber pressure, co-incident with temporary, sharp increases in upstream aerosol concentration believed to have arisen as a result of additional agitation of the fluidised-bed (Fig. 7(b)). Under these conditions, it is remarkable that plugging eventually occurred even at relatively high values of pressure differential (80 and 100 kPa), in contrast with the behaviour observed in tests in which such pressures were maintained from the start of aerosol exposure (Fig. 6).

In the final two tests, the capillaries were initially exposed to aerosol at the highest pressure differential studied (100 kPa), reducing in 20 kPa decrements to 40 kPa. The time-dependent variations in particle penetration for these capillaries are shown in Fig. 8(a) and

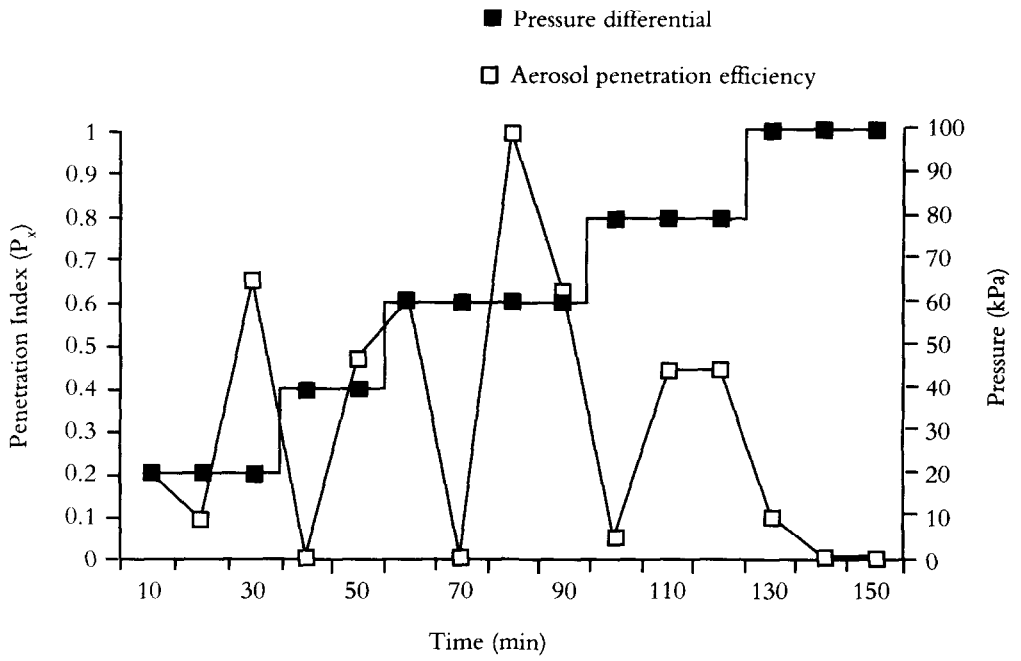

(a) Pressure variation and aerosol penetration behaviour

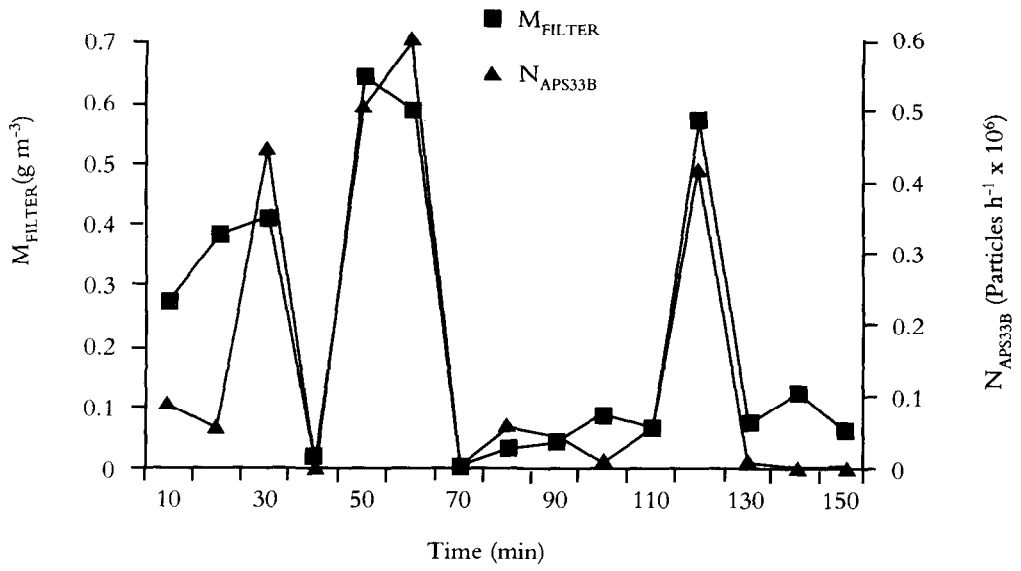

(b) Aerosol behaviour

Fig. 7. Aerosol penetration behaviour for stepped increases in pressure.

(b). In both cases, the particle penetration rate declined rapidly to zero as the pressure differential was reduced, even though the aerosol concentration in the exposure chamber remained at a significant level. The steady and irreversible decline in P_x was anticipated because in these cases there were no pressure-flow surges during adjustments of chamber pressure that might have unblocked the plugged capillaries.

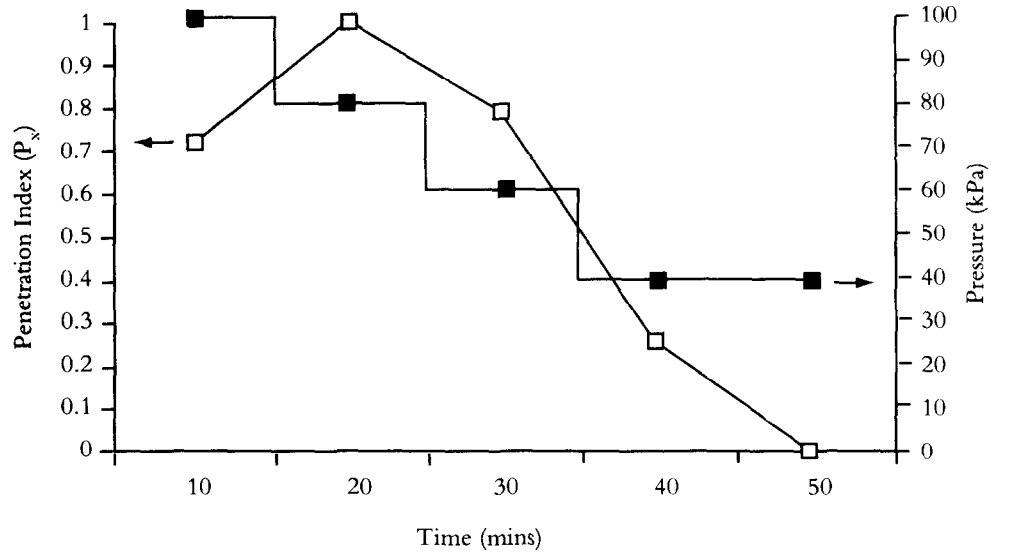

(a) First capillary

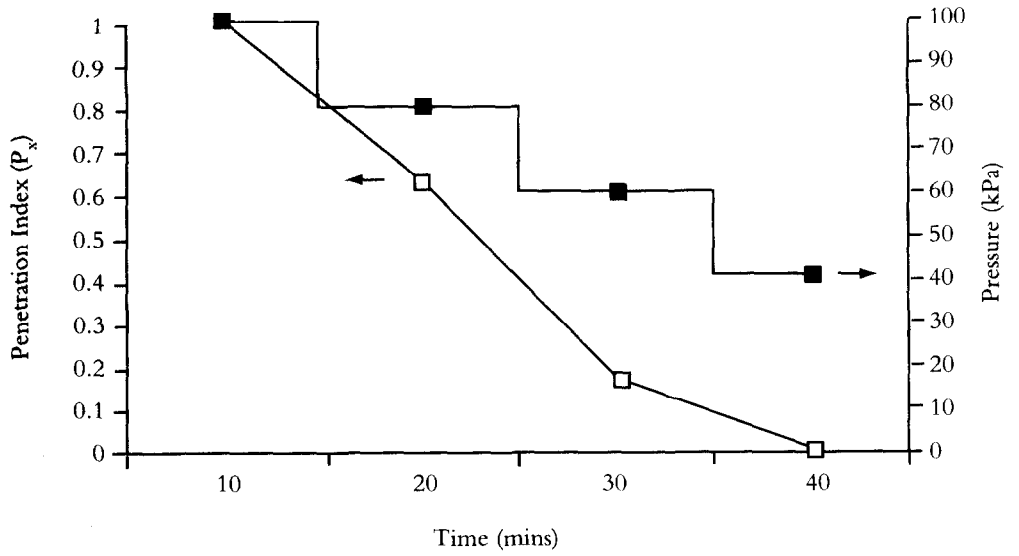

(b) Second capillary

Fig. 8. Aerosol penetration behaviour for stepped decreases in pressure.

Post-test examination of capillaries

Post-test examination of the capillary entrances by microscopy revealed that the entrances were covered with a deposit of glass microspheres, as can be seen from a comparison of photomicrographs of an unused capillary (Fig. 9(a)) with the entrance of a capillary that had been tested at a pressure differential of 20 kPa (Fig. 9(b)). It was not always possible to distinguish between plugged and un-plugged capillaries in this way, although there was qualitative evidence that less deposition had occurred in the cases of capillaries that had only been exposed to aerosol at relatively high values of pressure differential.

(a) Unused capillary

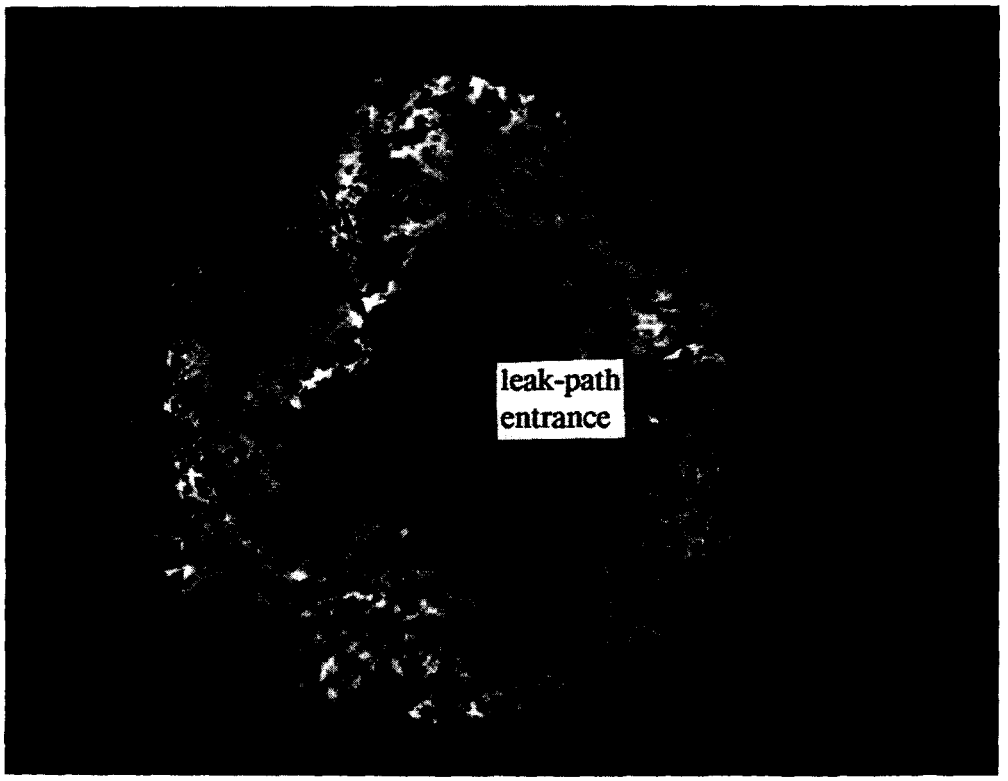

(b) Plugged capillary showing particle deposit at entrance to leak-path

Fig. 9. Photomicrographs of capillary entrances.

DISCUSSION

Clement (1993) has argued from first principles that ultra-fine leak-paths with dimensions slightly larger than the diameter of the particles will eventually plug as impaction and sedimentation result in the accretion of deposits near the entrance and on internal surfaces. The motion of micron-sized particles is comparatively unaffected by other processes such as Brownian diffusion, although it is recognised that electrostatic charging may have a profound influence on deposition behaviour. However, if electrostatic effects are neglected, an important finding from the model of capillary leakage is that the total mass of particulate leaked at a given pressure differential before blockage occurs should be independent of the upstream aerosol concentration. Thus, the need to establish the behaviour of the aerosol within the leaking container may be avoidable, and instead efforts should be directed to the measurement of the total mass of particulate leaked. Unfortunately, the situation becomes more complex if the driving pressure varies, as short-term pressure surges can modify the transport and deposition behaviour of micron-sized particles into and through the leak-path by affecting particle inertia, as well as initiating the breakdown of partly or fully formed plug-like deposits. Changes in deposition behaviour are bound to have a major effect on the total mass of particulate leaked, and in some instances, plugging may not occur if resuspension processes dominate to prevent the accumulation of deposited particles.

In these experimental studies, there is strong evidence from post-test examination of the capillaries by microscopy that plugging occurred at or close to the entrance (located in the pressure chamber), and was most rapid when the pressure differential was low. In a few cases, it appeared that incipient plug formation could be prevented by increasing the pressure differential. However, any increase in particle emission from the cleared leak-path was temporary, and plug formation continued at the new conditions.

It is recognised that repeat tests at selected conditions are required to substantiate the observations of what is a stochastic process, before reliable predictions can be made about aerosol leakage behaviour under the influence of pressure variations. In particular, it would be helpful if the upstream aerosol concentration could be maintained at a constant value to eliminate this complicating factor. Despite these limitations, it is still possible to make observations concerning the effect of pressure on aerosol leakage behaviour that are consistent with the experimental data.

Firstly, the local aerosol deposition velocity at the entrance to the capillary appeared to increase when the pressure differential across the leak-path was reduced within the range studied, enhancing the rate at which particles collected at this location. At first sight, this observation might appear to conflict with intuition: increased deposition might be expected at high pressure differentials, due to the increased particle velocity (inertia) in the converging flow near to the capillary entrance. However, deposit fragmentation and particle resuspension are also more likely at higher flow velocities. Both effects counter the formation of deposits at the capillary entrance and offset deposition to internal surfaces by sedimentation, and would therefore result in continued aerosol leakage as observed in this studies.

Secondly, it might have been expected that the air leakage rates measured after each test would have been zero in cases in which particle penetration rates had decreased to zero during exposure to the aerosol. In several cases (for instance, the capillaries exposed to aerosol at fixed pressure differential values of 20 and 40 kPa), post-test air leakage rates were still significant (in the latter case almost the same as the pre-test measurement), despite evidence from particle penetration measurements and post-test examination by microscopy that the entrances to both capillaries had plugged. It is possible that any plug formed during exposure to the aerosol may have become dislodged before the post-test air leakage rate was measured. However, the effect occurred on many occasions and a more likely explanation seems to be that the aerosol debris may have acted as filters, allowing the passage of air but preventing further particle ingress.

The following processes are proposed to describe the observed behaviour.

(1) Initial deposition took place in a narrow rim around the entrance to the capillary.
(2) Further deposition took place by inertial interception onto previously collected

particles, resulting in bridge formation as deposits on either side of the entrance to the capillary linked up.

(3) The dendrite-like growths of deposited particles at the capillary entrance (observed by microscopy at high magnification) acted as a filter, removing further incoming particles by inertial interception, while permitting the free passage of the air flow (compare SLR values before and after aerosol exposure for many of the capillaries (Table 1)).

(4) The thickness of the deposit will eventually increase to the point at which the air flow through the leak-path diminishes to zero (this condition was never attained in these experiments, although significantly reduced SLR values after aerosol exposure were observed in cases where the capillaries were tested at 20 or 40 kPa (Table 1)).

CONCLUSIONS

Previous studies of the leakage of sub-micron- and micron-sized aerosols through ultra-fine capillaries have been extended to quantify the effect of varying the upstream pressure on particle transport behaviour. The following conclusions can be drawn from these tests.

(a) At relatively high pressure differentials across the capillary on test ($\geqslant 80$ kPa), there was little evidence that particle deposition occurred to an extent that resulted in significant blockage of the leak-path. Such behaviour had been observed in previous work conducted at a pressure close to 100 kPa (Mitchell *et al.*, 1990). Variations in the APS33B-measured particle penetration rate (particles h^{-1}) followed fluctuations in aerosol mass-concentration in the pressure vessel as measured by the filter-collection technique.

(b) When the pressure differential was reduced, there was strong evidence that aerosol leakage was attenuated; this process appeared most rapid in cases where the pressure differential was at relatively low (20 kPa); no penetration occurred after approximately 10 min exposure to aerosol under these conditions. Aerosol attenuation also occurred in cases where the capillary had been tested initially at low pressure, even when the pressure differential was subsequently raised above 60 kPa.

(c) Microscopic inspection of the capillaries after each test in which significant aerosol attenuation had occurred, demonstrated that large numbers of particles had deposited at the entrance to the capillaries and facing the aerosol source in the pressure chamber. These deposits appear to have formed a filter-like barrier, that limited further particle penetration.

(d) Measurements of post-test air leakage through several capillaries demonstrated that in the early stages of deposit formation there was little (if any) reduction in the air leakage rate, despite evidence from the APS33B-measured penetration rates that significant aerosol attenuation had occurred during exposure.

(e) Changes in the pressure differential across these capillary leak-paths may have influenced the particle deposition rate at the entrance by modifying local velocity gradients associated with the converging flow. Deposition velocities appear to have been enhanced at a relatively low pressure differential; at the same time, shear forces that might have disrupted the formation of plug-like structures would have been minimal in strength.

These studies have demonstrated that the driving pressure (pressure differential) across an ultra-fine leak-path is of fundamental importance in determining the mass of aerosol that might penetrate the defective seal of a transport container. Thus the thermal-hydraulic conditions within the container at the time of the potential leak are likely to have a profound influence on whether rapid plugging takes place, and limit the egress of particles. Plugging of the leak-path appears likely to be more rapid when the driving pressure is low and the breach is of similar dimensions to the diameters of the aerosol particles.

It must be emphasised that these tests were preliminary in nature and limited to straight leak-paths. Further, testing with leak geometries more realistic to those encountered with transport container seals is required to demonstrate the conservative nature of the assumption that particle penetration at a given SLR is most severe when the leak-path is straight. In particular, the exact shape of the entrance is likely to have an important bearing on the location of subsequent deposition in the leak-path.

Acknowledgements—The authors wish to thank A. C. Burton (AEA Technology) for undertaking much of the experimental work. They also wish to thank C. F. Clement, J. Higson, A. L. Nichols, and P. J. Stopford (all of AEA Technology) for technical advice. This work was funded by the Nuclear Materials Management Programme Letter of the U.K. Department of Trade and Industry, administered by AEA Technology and the Commission of the European Communities (Contract 4.1020/E92-01).

REFERENCES

AEA Technology (1992) Transport of radioactive material code of practice: leakage tests on packages for transport of radioactive material. AECP 1068, AEA Technology, Harwell.

Ball, M. H. E., Marshall, I. A., Mitchell, J. P. and Rideal, G. R. (1989) An assessment of glass microspheres for use as number-based aerodynamic size standards. AEA Technology Report AEEW-R 2544, Winfrith.

Burrows, G. (1961) Flow through and blockage of capillary leaks. *Trans. Inst. Chem. Engrs* **39**, 55–63.

Burton, A. C., Mitchell, J. P. and Morton, D. A. V. (1993) The influence of pressure on the penetration of aerosols through fine capillaries. *J. Aerosol Sci.* **24** (Suppl. 1), 559–560.

Clement, C. F. (1993) Aerosol penetration through capillaries and leaks. *Proc. 7th Ann. Conf. of the Aerosol Society*, pp. 8–11. The Aerosol Society, Portishead, Bristol.

Curren, W. D. and Bond, R. D. (1980) Leakage of radioactive powders from containers. *Proc. Int. Symp. on the Packaging and Transportation of Radioactive Materials, PATRAM 80*, pp. 463–471. K. O. Storke & Co., Berlin.

Hinds, W. C. (1982) *Aerosol Technology*. Wiley, New York.

International Atomic Energy Agency (1985) Regulations for the safe transport of radioactive material. Safety Series No. 6, STI/PUB/691 IAEA, Vienna.

Marple, V. A., Liu, B. Y. H. and Rubow, K. L. (1978) A dust generator for laboratory use. *Am. Ind. Hyg. Assoc. J.* **39**, 26–32.

Mitchell, J. P., Edwards, R. T. and Ball, M. H. E. (1990) The penetration of aerosols through fine capillaries. *Int. J. Radioactive Materials Transport* **1**(2), 101–116.

Mitchell, J. P., Morton, D. A. V. and North, B. M. (1992) The penetration of sub-micron non-spherical particles through ultrafine capillaries. AEA Technology Report AEA-EE-0361, Winfrith.

Morton, D. A. V., North, B. M. and Mitchell, J. P. (1992) The penetration of micron-sized non-spherical particles through ultrafine capillaries. AEA Technology Report AEA-EE-0301, Winfrith.

Remiarz, R. J., Agarwal, J. K., Quant, F. R. and Sem, G. J. (1983) Real-time aerodynamic particle sizer. *Aerosols in the Mining and Industrial Work Environments* (Edited by Marple, V. A. and Liu, B. Y. H.), pp. 879–895. Ann Arbor Science, Ann Arbor, MI.

Stopford, P. J. and Williams, M. G. (1992) The modelling of aersol deposition in ultrafine capillaries. AEA Technology Report AEA-D&R-0377, Harwell.